

AD-A160 746

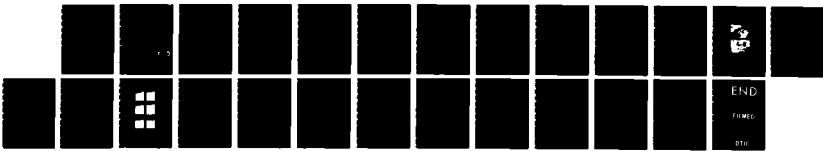
SURFACE CREEP OF MINERAL OIL ON INNER RING OF MOMENTUM
WHEEL BEARING (U) AEROSPACE CORP EL SEGUNDO CA
CHEMISTRY AND PHYSICS LAB P D FLEISCHAUER ET AL

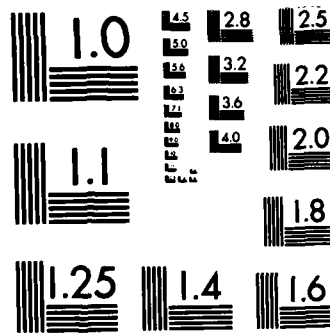
1/1

UNCLASSIFIED

19 AUG 85 TR-0084A(5945-03)-1 SD-TR-85-52 F/G 11/8

NL





MICROCOPY RESOLUTION TEST CHART
NATIONAL BUREAU OF STANDARDS-1963-A

12

REPORT SD-TR-85-52

AD-A160 746

Surface Creep of Mineral Oil on Inner Ring of Momentum Wheel Bearing

PAUL D. FLEISCHAUER and H. DANIEL MARTEN
Chemistry and Physics Laboratory
Laboratory Operations
The Aerospace Corporation
El Segundo, CA 90245

19 August 1985

APPROVED FOR PUBLIC RELEASE;
DISTRIBUTION UNLIMITED

DTIC FILE COPY

DTIC
ELECTE
OCT 28 1985
S D
E

Prepared for
SPACE DIVISION
AIR FORCE SYSTEMS COMMAND
Los Angeles Air Force Station
P.O. Box 92960, Worldway Postal Center
Los Angeles, CA 90009-2960

85 10 28 021

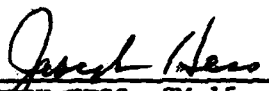
This report was submitted by The Aerospace Corporation, El Segundo, CA 90245, under Contract No. F04701-83-C-0084 with the Space Division, P.O. Box 92960, Worldway Postal Center, Los Angeles, CA 90009-2960. It was reviewed and approved for The Aerospace Corporation by S. Feuerstein, Director, Chemistry and Physics Laboratory. Lieutenant Buford W. Shipley, Jr., SD/YDEA, was the project officer for the Mission-Oriented Investigation and Experimentation (MOIE) program.

This report has been reviewed by the Public Affairs Office (PAS) and is releasable to the National Technical Information Service (NTIS). At NTIS, it will be available to the general public, including foreign nationals.

This technical report has been reviewed and is approved for publication. Publication of this report does not constitute Air Force approval of the report's findings or conclusions. It is published only for the exchange and stimulation of ideas.



BUFORD W. SHIPLEY, JR., Lt, USAF
MOIE Project Officer
SD/YDEA



JOSEPH HESS, GM-15
Director, AFSTC West Coast Office
AFSTC/WCO OL-AB

SECURITY CLASSIFICATION OF THIS PAGE(When Data Entered)**19. KEY WORDS (Continued)****20. ABSTRACT (Continued)**

raceway (the balls were not present). The oil was observed to migrate up the curved surface until it reached the corner of the raceway. A bead of oil would form at that corner. In no case did oil actually creep across the land. The oil bead thickness was a function of speed, but at 9000 rpm should be approximately 0.12 mm (0.005 in.).

PREFACE

The authors thank M. A. Rocha for designing and constructing the test fixture and for his contributions to the experimental portion of the project, and Dr. P. A. Bertrand for assisting with the analysis of the surface tension effects.

Accession For	
NTIS GRA&I	<input checked="" type="checkbox"/>
DTIC TAB	<input type="checkbox"/>
Unannounced	<input type="checkbox"/>
Justification	
By _____	
Distribution/	
Availability Codes	
Dist	Avail and/or Special
A-1	



CONTENTS

PREFACE.....	1
I. INTRODUCTION.....	7
II. EXPERIMENTAL PROCEDURES.....	9
A. Lubricants.....	9
B. Test Fixture.....	9
C. Bearing.....	12
D. Test Sequence.....	12
III. RESULTS AND DISCUSSION.....	15
IV. CONCLUSIONS.....	23
REFERENCES.....	25

FIGURES

1.	Schematic of apparatus for measuring lubricant migration.....	10
2.	Fixture for measuring lubricant creep.....	11
3.	Photographs of spinning bearing ring showing luminescence of KG 80 (oil C).....	16
4.	Sketch of forces and geometry involved in deriving Eqs. (1) through (5).....	17
5.	Plots of lubricant bead diameter versus speed of rotation for series of oils.....	19
6.	Plot of bead diameter versus viscosity of oil for constant speed of 5000 rpm.....	21

TABLES

1.	Lubricant Properties.....	10
2.	Bearing Specifications.....	13

I. INTRODUCTION

Satellite stabilization systems, such as momentum wheels, require highly reliable bearing systems that operate unattended for long times at high speeds. To achieve such performance, lubricant feed systems have been developed that operate on the centrifuge principle. Oil is forced from reservoirs through a delivery system into the spinning bearings. The oil flows in an outward, radial direction, and the feed rate is determined by the bearing's speed of rotation and the degree of complexity of the tortuous path that the oil takes to get to the bearing. The oil feed rate must be sufficient to replenish oil lost by evaporation, by outward motion induced by rotation speed, and by creep. Lubricant creep can be especially important if there are temperature gradients within a system^{1,2} or if creep is an important mechanism for the proper lubrication of the bearing. The purpose of this study was to measure the creep of oil for a spinning bearing ring and to determine the extent of oil creep from the ball track up to and across the land surface.

II. EXPERIMENTAL PROCEDURES

The creep of oil from the bearing raceway surface onto the land was investigated, using the fact that additives in the oil fluoresce under ultraviolet excitation. A fixture was designed and constructed so that this fluorescence could be monitored photographically while the inner ring of the bearing of interest was spinning at speeds up to 7000 rpm.

A. LUBRICANTS

The lubricants employed for these measurements were from a series of superrefined base stocks originally prepared from a paraffinic crude oil and blended with a proprietary additive package that contains, among other components, tricresyl phosphate antiwear additive, which was also coated on the bearing part according to standard procedures prior to use. Properties of the oils are given in Table 1.

B. TEST FIXTURE

The test fixture, shown schematically in Fig. 1 and photographically in Fig. 2, consisted of a belt-driven shaft upon which the bearing inner ring was press fit and a vacuum chamber that was constructed to spin along with the bearing during testing. A plastic tube sealed to aluminum end plates by means of O-rings formed the chamber; it could be evacuated to approximately 1.33×10^{-2} Pa with a rotary vane pump prior to test. The plastic tube was transparent to the near-ultraviolet excitation light from a 100-W high-pressure mercury arc lamp. The lamp output was filtered through a 20-mm water filter and a glass filter that transmitted a band in the wavelength region from approximately 280 to 390 nm. The emission of the lubricant could be seen easily and was recorded photographically with a 35-mm camera mounted on a copy stand. The entire chamber, including the bearing, could be rotated at speeds ranging from 0 to 7000 rpm, the upper limit being imposed by the yield strength of the plastic tube. The speed of rotation was measured with a photoelectric tachometer that sensed the driven gear of the chamber. A spring-loaded wick apparatus, shown in Fig. 2b, applied oil to the spinning

TABLE 1. LUBRICANT PROPERTIES

PROPERTY	PARAFFINIC BASE OILS			
	A (SRG 40)	B (SRG 60)	C (KG 80)	D (SRG 160)
Density, ^a g·L ⁻¹	843.3	856.7	831.7	818.8
Viscosity, ^a mm ² ·s ⁻¹ at 23°C	54	214	420	1420
Viscosity index ^b		106	101	107
Pour point, ^b °C		-12	-9.4	-7
Flash point, ^b °C		232	274	302

^aMeasured in our laboratory.

^bTaken from manufacturer's specifications.

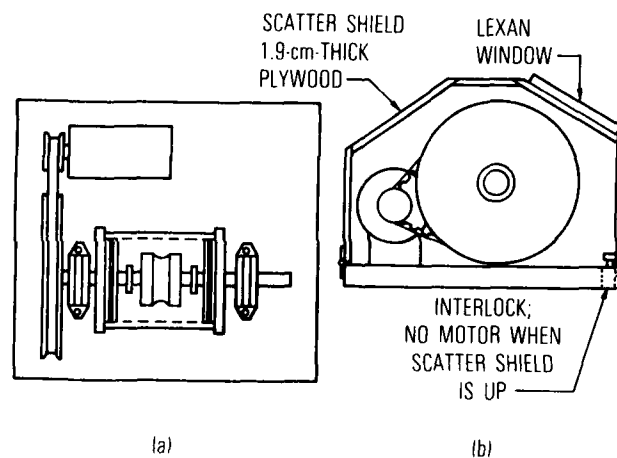
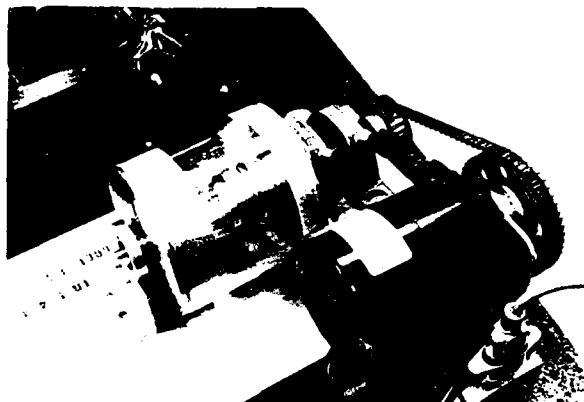
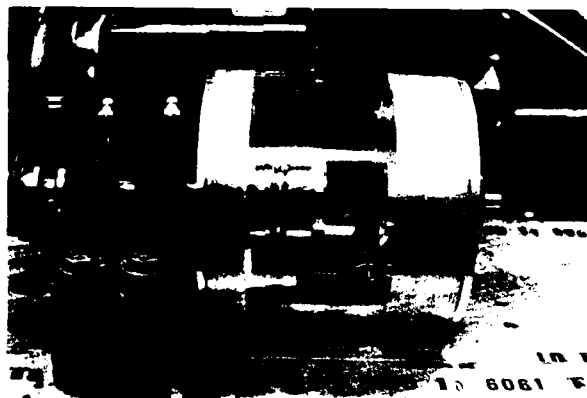


Fig. 1. Schematic of apparatus for measuring lubricant migration: (a) top view; (b) side view (side panel removed to show detail).



(a)



(b)

Fig. 2. Fixture for measuring lubricant creep: (a) top view; (b) front view, showing wick apparatus at lower right in cylinder.

raceway during rotation. It was weighted and connected to the end plate by a ball bearing so that it remained at the bottom of the chamber throughout operation.

C. BEARING

The test item was the inner ring from a flight-quality, angular contact, deep groove, momentum-wheel ball bearing, detailed in Table 2.

D. TEST SEQUENCE

The test sequence consisted of lubricating the bearing with a very thin coat of oil, applying oil to the wick, evacuating the chamber, and photographing the luminescence of the oil at various speeds of rotation. Before each sequence, the bearing was cleaned in an ultrasonic cleaner with heptane as solvent. The initial coat of oil was applied by wiping a 1:50 solution of oil in Freon TF over the surface. The wick was rinsed with heptane and dried, then neat oil was applied with a capillary dropper. The test chamber was pumped through a swage-type fitting that contained a Teflon plug for sealing the chamber at the pumping opening when the pressure reached the 1.33×10^{-2} Pa range. After the Teflon plug was seated, the connection to the vacuum pump was removed so that there would be no encumbrances to chamber rotation.

A photograph of the bearing was taken before rotation began, as a reference for subsequent measurements of the oil bead thicknesses. The width of the bearing relief was used for this reference. All photos in a series were printed at the same focal setting to avoid introducing errors from the optics of the photographic process.

The fixture was then rotated at a speed of 3000 rpm and photographed. The speed was increased in increments of 1000 rpm until the 7000-rpm limit was reached. In at least one case with KG 80 (oil C) the sequence was reversed; that is, the high speed was photographed first and then the speed was decreased in 1000-rpm increments.

TABLE 2. BEARING SPECIFICATIONS

Tolerances	ABEC 9
Material	SAE 52100 (C.E.V.M.)
Size	107
Land diameter	43.434 mm
Race diameter	40.5638 mm
Pitch diameter	48.514 mm
Groove radius	4.087 mm
Inner diameter	35.000 mm

III. RESULTS AND DISCUSSION

Figure 3 is a set of sample photographs. Figure 3a shows the bearing before rotation; Figs. 3b through 3f show the bearing at 3000 through 7000 rpm. From the photographs, it is apparent that oil creeps up the curved surface until it reaches the corner at the beginning of the land surface, at which point a bead of oil forms, its width (diameter) decreasing with increasing rpm. There appears to be a very slight movement of the oil beyond the corner, equivalent to the bead diameter, but there is no creep across the land. The oil accumulates at the corner of the race as a result of the high surface-tension forces exerted at this curved surface.³ After sufficient oil has accumulated in the bead, the dynamic (centrifugal) force acting on the oil mass exceeds the surface tension and oil is thrown off the ring in an outward radial direction to be collected on the chamber wall (plastic tube). The illumination, light filtering, and focusing obscure this effect in Fig. 3, but it was clearly visible during the experiments.

The diameter that the oil bead assumes will be determined by the balancing of the dynamic and surface tension (adhesion) forces. An attempt was made to derive equations for describing the action of surface tension and of radial forces by assuming a specific, constant drop shape for all speeds: a semicircular cross section. (See Fig. 4b.) The surface tension portion of this relationship is usually expressed as the "work of adhesion":

$$W_A = \gamma_A + \gamma_B - \gamma_{AB} \quad (1)$$

where γ_A is the surface tension of the oil, γ_B that of the substrate, and γ_{AB} that of the oil-substrate interface.⁴ One way of equating the work of adhesion and the dynamic action is to express the dynamic portion as kinetic energy. The equilibrium bead size will exist when the work of adhesion is equal to the kinetic energy within the oil bead:

$$W_A (2\pi R d) = \frac{m R^2 \omega^2}{2} \quad (2)$$

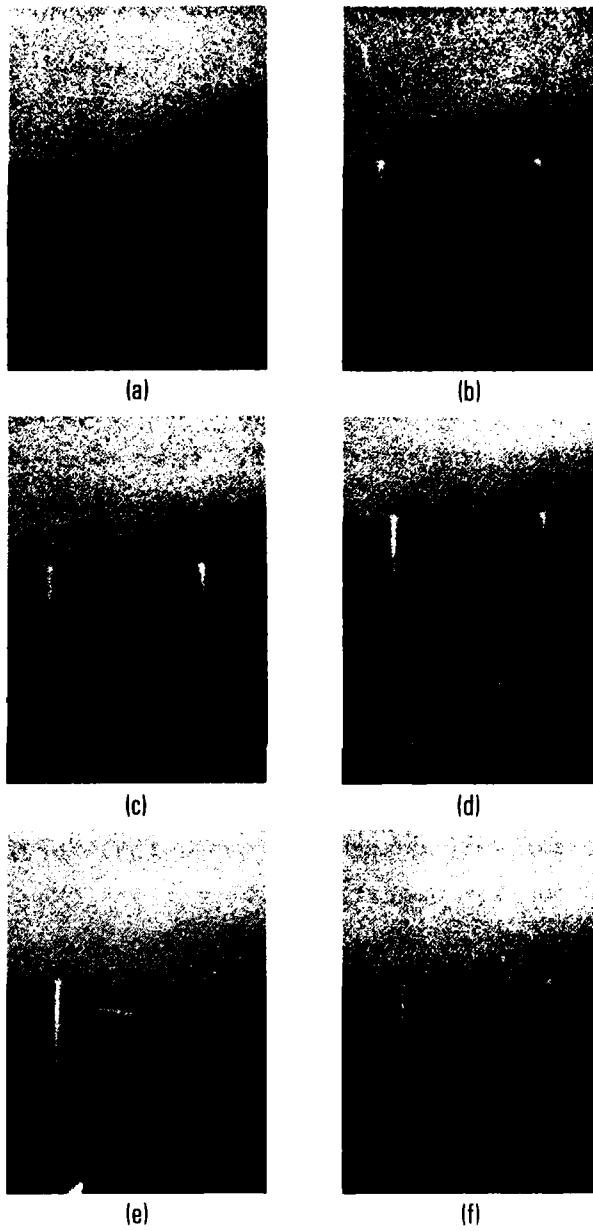


Fig. 3. Photographs of spinning bearing ring showing luminescence of KG 80 (oil C): (a) 0 rpm; (b) 3000 rpm; (c) 4000 rpm; (d) 5000 rpm; (e) 6000 rpm; (f) 7000 rpm.

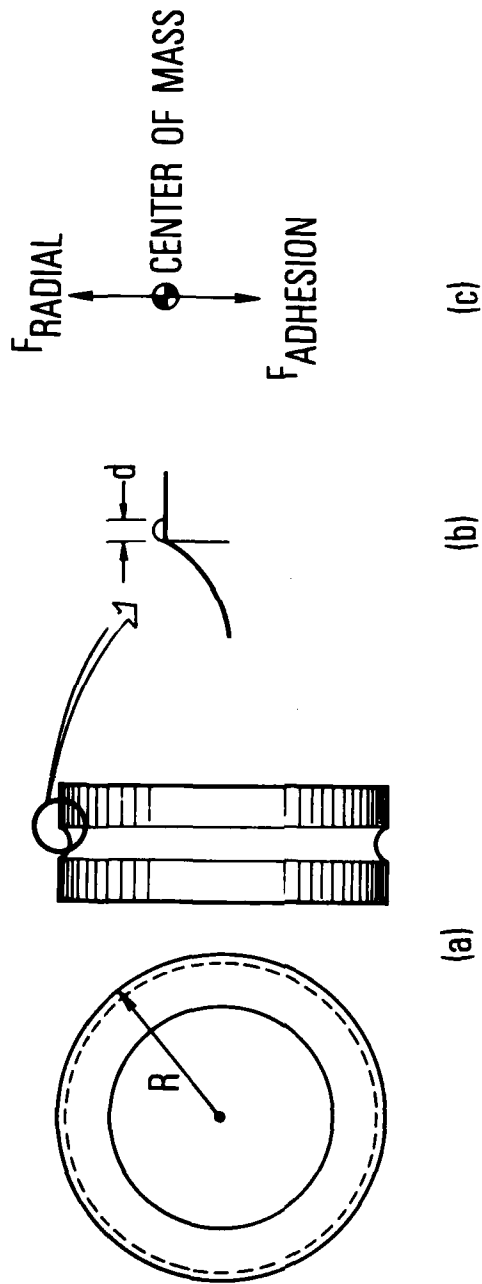


Fig. 4. Sketch of forces and geometry involved in deriving Eqs. (1) through (5): (a) bearing radius R and cross section; (b) cross section of oil bead on bearing land; and (c) free-body diagram of oil cross section.

where W_A is multiplied by the area of contact of the oil bead, R is the bearing radius, d is the oil bead width, and w is the bearing rotational velocity. (See Figs. 4a and 4b.) The mass of oil in the bead, m , must be expressed in terms of the volume of oil in the bead:

$$m = \frac{\rho \pi R d^2}{4} \quad (3)$$

where ρ is the density of the oil. Substituting Eq. (3) into Eq. (2) gives

$$2W_A = \frac{\rho \pi R^2 d w^2}{8} \quad (4)$$

For a given oil and substrate (bearing steel), all of the terms in Eq. (4) are constant except for d and w . Therefore,

$$d w^2 = \text{constant} \quad (5)$$

Alternatively, the surface tension can be expressed as a force per unit length instead of work per unit area, and then equated with the dynamic radial (centrifugal) force per unit length around the circumference. (See Fig. 4c.) Either way, one obtains the relationship that the diameter of the oil bead multiplied by the square of the rotational speed is a constant, or that the diameter of the bead is inversely proportional to the speed squared, as the plots of bead thickness versus rotation speed in Fig. 5 demonstrate. The dashed line in the plot for oil C shows the fit of our data to such a relationship, where the "theory" and experimental results were force fit (normalized) at a speed of 5000 rpm. Although the data appear to fit a linear relationship equally well, the quadratic expression was used to extrapolate an estimated bead diameter for higher speeds. Thus, the data and the expected relationship combine to give an estimate that should be better than that using either the data or mathematical relationship alone. A speed of 9000 rpm was of interest for this work; the estimated bead thicknesses for this speed are as follows:

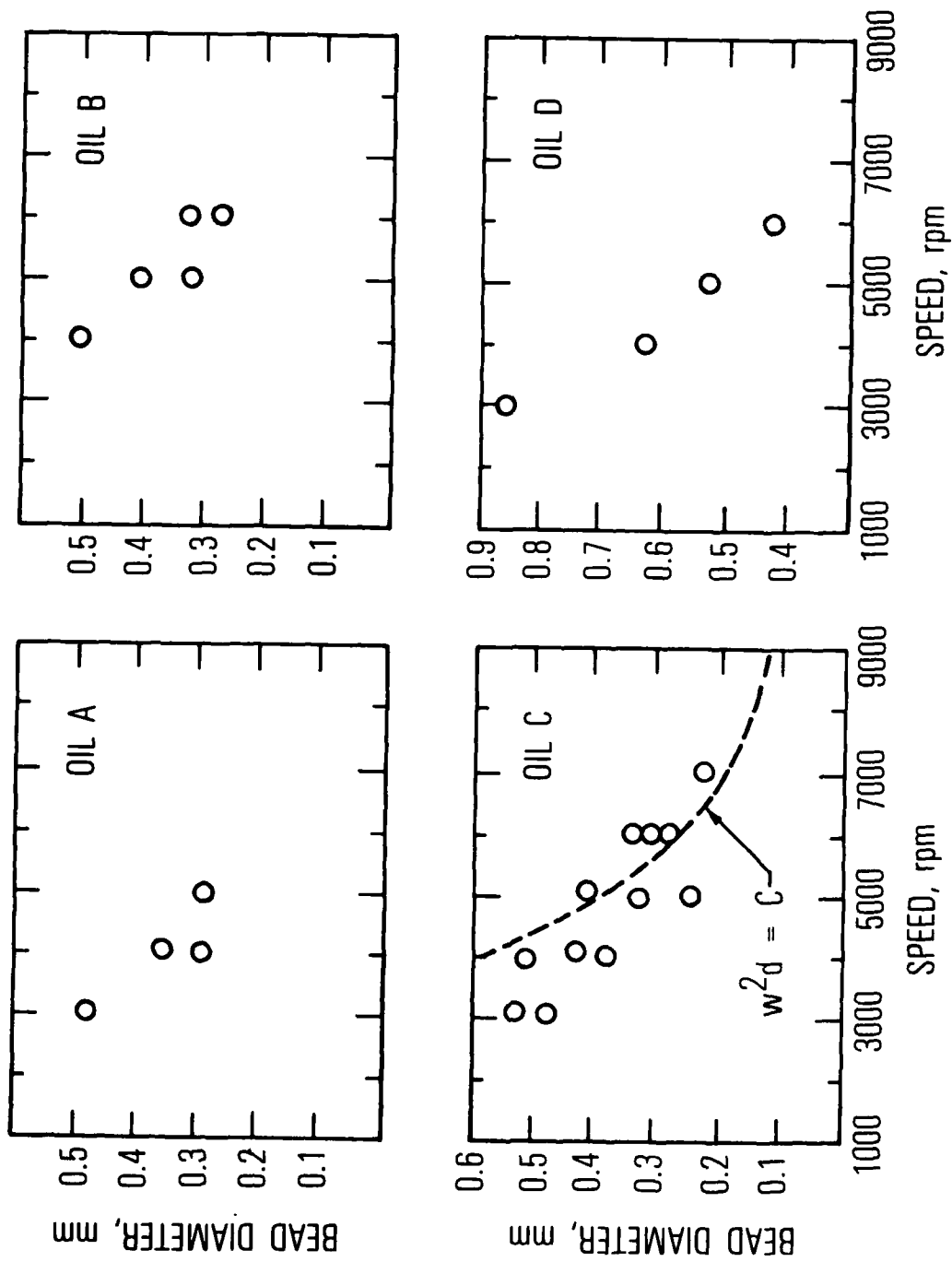


Fig. 5. Plots of lubricant bead diameter versus speed of rotation for series of oils. (See Table 1.)

Oil A	0.09 mm
Oil B	0.11 mm
Oil C	0.12 mm
Oil D	0.16 mm

The variation in oil bead thickness as a function of bearing operating temperature is also of concern for certain applications. Two properties of a fluid lubricant, the viscosity and the surface tension, are temperature dependent. Experimental constraints prevented making measurements at different temperatures; however, temperature effects can be assessed from consideration of the experimental data for the different viscosity oils and of literature data on the effects of temperature on surface tension. From the data of Fig. 5, the trend of decreasing bead thickness with increasing rpm is evident for all four oils. The lowest-viscosity oil (A) displayed very weak fluorescence; therefore, at the highest speed (7000 rpm), no emission could be detected. There is a weak correlation between the thickness of the oil bead measured at a given speed and the oil viscosity, as shown in Fig. 6 for 5000 rpm, with the higher-viscosity oils tending to exhibit slightly wider beads or slightly greater accumulation before being thrown off the race. The density variation of the oils, listed in Table 1, is not monotonic, so the observed trend does not appear to be density dependent.

The viscosity of oil C changes from $420 \text{ mm}^2 \cdot \text{s}^{-1}$ (centistokes) to $225 \text{ mm}^2 \cdot \text{s}^{-1}$ for a 10°C change from 23°C to 33°C , a change approximately equivalent to the difference between oil C and oil B at 23°C . Therefore, one can conclude that the minimum decrease in bead thickness for oil C for this 10°C increase would be the approximate 10-percent change shown in Fig. 6 for changing from oil C to oil B.

The temperature of operation of a bearing will also affect the surface tension of the oil on the metal surfaces. The temperature coefficient of the surface tension variation for a typical oil is of the order of $-0.1 \text{ dyne} \cdot \text{cm}^{-1} \cdot \text{C}^{-1}$; the higher the temperature, the lower the surface tension.^{1,5} A typical value of the surface tension for a superrefined paraffinic oil

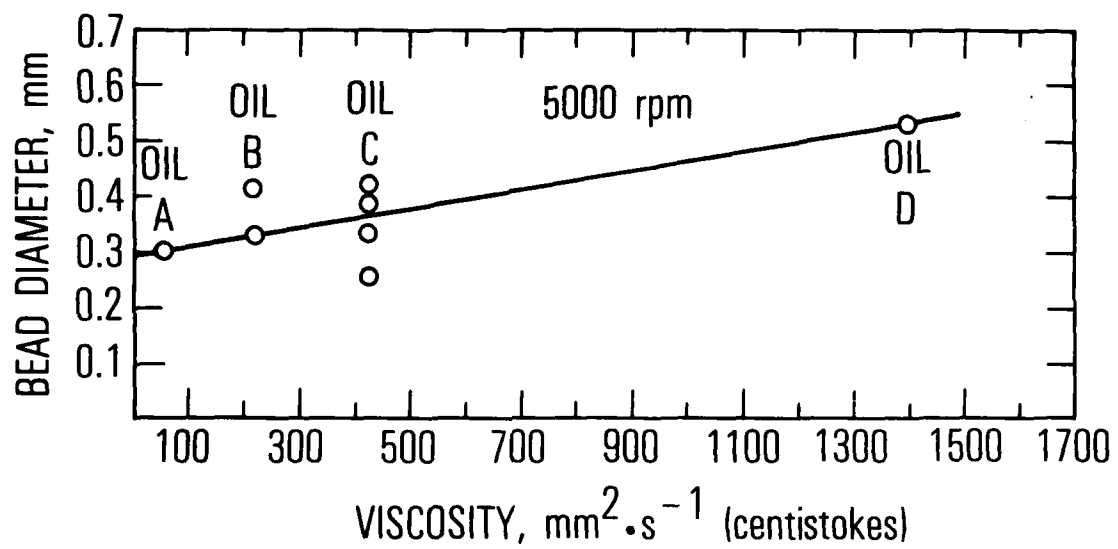


Fig. 6. Plot of bead diameter versus viscosity of oil for constant speed of 5000 rpm.

is $30 \text{ dyne}\cdot\text{cm}^{-1}$, so the above-mentioned change in temperature would cause an approximate 3-percent change in surface tension. Because the bead thickness is directly proportional to surface tension, a corresponding 3-percent change in bead thickness would be predicted. The temperature-induced changes in bead thickness for both viscosity and surface tension parameters are in the same direction—a decrease in bead thickness for an increase in temperature—and the magnitudes of the changes due to both effects are comparable.

For very long lifetimes of operation in vacuum, the low-molecular-weight portions of an oil generally evaporate; leaving the heavier, more viscous portions. The bead thickness for a migrating oil under such conditions would be expected to be thicker because of the increased viscosity compared with that at the beginning of life. However, in the present case the variation in viscosity of the superrefined oil would be very small; consequently, any change in creep characteristics would also be very small.

IV. CONCLUSIONS

Our measurements of lubricant creep on a spinning, high-speed ball-bearing race yield the following conclusions:

1. Oil will creep from the ball track "up" the curved portion of the race as a result of radial forces on the oil.
2. Oil will not creep across the flat land of the ring but, instead, will accumulate at the corner where curve and flat meet, and then be thrown off the ring in a radial direction.
3. The volume of oil that accumulates at the corner decreases with increasing speed of rotation and with increasing temperature at constant speed.
4. A reasonable approximation of the variation in the volume of oil accumulated as a function of rotation speed can be made by balancing the surface tension forces and the dynamic (centrifugal) forces for the spinning ring.
5. The temperature effects of viscosity and surface tension are comparable (i.e., of the same order of magnitude).

REFERENCES

1. A. A. Fote, L. M. Dormant, and S. Feuerstein, "Migration of Hydrocarbon Oil on Metal Substrates under the Influence of Temperature Gradients," Lubr. Eng. 32, 542-545 (1976).
2. A. A. Fote, R. A. Slade, and S. Feuerstein, "Thermally Induced Migration of Hydrocarbon Oil," J. Lubr. Technol. 99, 158-162 (1977).
3. A. A. Fote, R. A. Slade, and S. Feuerstein, "The Prevention of Lubricant Migration in Spacecraft," Wear 51, 67-75 (1978).
4. A. W. Adamson, Physical Chemistry of Surfaces, 4th ed., John Wiley and Sons, New York (1982), p. 64.
5. W. R. Jones, Jr., and L. D. Wedeven, "Surface-Tension Measurements in Air of Liquid Lubricants to 200°C by the Differential-Maximum-Bubble-Pressure Technique," NASA TN D-6450.

LABORATORY OPERATIONS

The Laboratory Operations of The Aerospace Corporation is conducting experimental and theoretical investigations necessary for the evaluation and application of scientific advances to new military space systems. Versatility and flexibility have been developed to a high degree by the laboratory personnel in dealing with the many problems encountered in the nation's rapidly developing space systems. Expertise in the latest scientific developments is vital to the accomplishment of tasks related to these problems. The laboratories that contribute to this research are:

Aerophysics Laboratory: Launch vehicle and reentry fluid mechanics, heat transfer and flight dynamics; chemical and electric propulsion, propellant chemistry, environmental hazards, trace detection; spacecraft structural mechanics, contamination, thermal and structural control; high temperature thermomechanics, gas kinetics and radiation; cw and pulsed laser development including chemical kinetics, spectroscopy, optical resonators, beam control, atmospheric propagation, laser effects and countermeasures.

Chemistry and Physics Laboratory: Atmospheric chemical reactions, atmospheric optics, light scattering, state-specific chemical reactions and radiation transport in rocket plumes, applied laser spectroscopy, laser chemistry, laser optoelectronics, solar cell physics, battery electrochemistry, space vacuum and radiation effects on materials, lubrication and surface phenomena, thermionic emission, photosensitive materials and detectors, atomic frequency standards, and environmental chemistry.

Computer Science Laboratory: Program verification, program translation, performance-sensitive system design, distributed architectures for spaceborne computers, fault-tolerant computer systems, artificial intelligence and microelectronics applications.

Electronics Research Laboratory: Microelectronics, GaAs low noise and power devices, semiconductor lasers, electromagnetic and optical propagation phenomena, quantum electronics, laser communications, lidar, and electro-optics; communication sciences, applied electronics, semiconductor crystal and device physics, radiometric imaging; millimeter wave, microwave technology, and RF systems research.

Materials Sciences Laboratory: Development of new materials: metal matrix composites, polymers, and new forms of carbon; nondestructive evaluation, component failure analysis and reliability; fracture mechanics and stress corrosion; analysis and evaluation of materials at cryogenic and elevated temperatures as well as in space and enemy-induced environments.

Space Sciences Laboratory: Magnetospheric, auroral and cosmic ray physics, wave-particle interactions, magnetospheric plasma waves; atmospheric and ionospheric physics, density and composition of the upper atmosphere, remote sensing using atmospheric radiation; solar physics, infrared astronomy, infrared signature analysis; effects of solar activity, magnetic storms and nuclear explosions on the earth's atmosphere, ionosphere and magnetosphere; effects of electromagnetic and particulate radiations on space systems; space instrumentation.

END

FILMED

11-85

DTIC